Sustainable Structures
ISSN: 2789-3111 (Print); ISSN: 2789-312X (Online)
http://www.sustain-dpl.com/journal/sust
DOI: 10.54113/j.sust.2026.000099

ORIGINAL ARTICLE

Effects of the use of recycled concrete aggregate on compressive behavior of partially encased composite columns

Meftahul Ahsan*, Md. Tanzil Hawlader, Mahbuba Begum

Department of Civil Engineering, Bangladesh University of Engineering and Technology, Dhaka-1000, Bangladesh
*Corresponding Author: Meftahul Ahsan. Email: meftahulahsan@ce.buet.ac.bd

Abstract: Using recycled concrete aggregate (RCA) can offer significant sustainability benefits by reducing waste and lowering the environmental impact on construction. This study presents a series of tests on short partially encased composite (PEC) columns to investigate the effects of RCA on the compressive behavior of PEC columns cast with recycled aggregate concrete. A total of 15 PEC columns and three bare steel columns were tested under concentric axial compression loads. The test incorporated five RCA replacement ratios (0%, 25%, 50%, 75%, and 100%) and three link spacing-to-depth ratios (0.33, 0.5, and 0.67). The failure modes, load-strain behavior, load capacity, and ductility were assessed to evaluate the effects of the RCA replacement ratio and link spacing. The failure mode was similar for all the PEC columns: crushing of concrete, and buckling of steel flanges. The test results indicate that columns become more brittle when the RCA replacement ratio exceeds 50% since RCA contains microcracks. However, under concentric loading, the effects of the RCA replacement ratios on column strength were negligible across different link spacing. Incorporating RCA resulted in a maximum 6% drop in strength. An increase in link spacing reduced the ultimate load for all columns. The initial stiffness was also comparable for different RCA replacement ratios and link spacings. Increasing the RCA replacement ratio increased the strain at peak load, especially for smaller link spacings. The current design guidelines for PEC columns with natural aggregate concrete can be safely used to predict the capacity of the PEC columns incorporating RCA. These findings enhance sustainable building techniques by illustrating that RCA can be utilized efficiently in PEC columns without a considerable decline in strength and stiffness.

Keywords: partially encased composite columns, recycled concrete aggregate, steel-concrete composite structure, concentric load, transverse link

1 Introduction

The construction industry has increasingly focused on sustainability and environmental preservation in recent years. The growing need for natural aggregates, combined with swift urban development, has resulted in the exhaustion of natural reserves and an intensified environmental impact [1]. Consequently, recycling construction and demolition waste into recycled concrete aggregate (RCA) has surfaced as a viable, sustainable replacement for natural aggregates. RCA is created by crushing and processing demolished concrete structures, providing an eco-friendly and economical alternative for concrete manufacturing [2]. The findings from the life cycle assessment revealed that utilizing

Received: 30 January 2025; Received in revised form: 6 August 2025; Accepted: 29 August 2025

recycled aggregates can decrease greenhouse gas emissions by as much as 65% and reduce non-renewable energy consumption by up to 58% [3]. However, concrete's workability and compressive strength may be reduced when using RCA due to its higher water absorption and lower density [4]. RCA exhibits lower physical and mechanical properties than natural aggregate (NA) [5,6]. Mortar in RCA is primarily responsible for the variance in RCA characteristics. Because of the mortar, RCA has lower specific gravity, higher absorption, and weaker abrasion resistance than NA [7]. However, when the source concrete of RCA is stronger, a comparable compressive strength can be obtained [5,8–10].

A partially encased composite (PEC) column comprises an H-shaped steel section and concrete infill between the flanges. For thin-walled PEC columns, transverse links are connected at a regular spacing between the flanges of the steel section to enhance resistance against buckling of flanges. Numerous experimental studies have been performed to evaluate the behavior, failure modes, and ultimate capacity of thin-walled PEC columns subjected to concentric [11–15] and eccentric [16–18] axial compressive loads. The behavior of PEC columns built of fiber-reinforced concrete and high-strength concrete was examined by Prickett and Driver [18]. According to the study, compared to normal-strength concrete, high-strength concrete failed more abruptly, and the insertion of steel fibers enhanced the ductility of the concrete. The use of lightweight concrete in PEC columns has also been studied [19,20]. Pereira et al. [21] evaluate the structural behavior of the column by substituting the longitudinal reinforcement and transverse link with wire mesh under axial and cyclic loadings. Chen et al. [22] studied the effect of the arrangement of additional reinforcements and found that the effects of the arrangement on the strength and ductility were insignificant. The behavior of octagonal-shaped PEC columns has also been studied [23–26]. Research has been done on the application of PEC columns as boundary elements for steel plate shear wall [27–31]. Finite element models and numerical studies were developed to reproduce the performance of PEC columns under numerous loads [32–38]. A numerical model was developed to use equivalent steel sections for analyzing short PEC columns under concentric loading [39].

In recent years, RCA extracted from demolished concrete lumps (DCL) has been used in composite columns [40–47], which is an important step toward sustainable development. In concrete-filled steel tubular (CFST) columns subjected to axial compression, less than 10% of the capacity was lost when recycled aggregates replaced 100% of the natural aggregates [45,46]. The overall structural behaviors of the CFST column were not much affected, even with up to 40% replacement of NA by RCA [40,42]. For the PEC column, Wu et al. [44] investigated the use of DCL on PEC columns. The experimental study used an RCA replacement ratio of up to 33% from two different sources. The large-sized DCLs were used for aggregate. The failure behavior of the columns containing RCA and the columns cast with NA were found similar. Also, the source of DCLs did not affect the failure pattern. The available study on using various percentages of RCA in PEC columns with variable geometric properties is very limited. The effects of RCA on the performance of these columns, especially under concentric and eccentric loading scenarios, have yet to be comprehensively examined. The behavior of columns with normal-sized RCA has also not been explored. The impact of RCA on the composite action between the steel section and the concrete core in PEC columns has received little consideration. In addition, the contribution of transverse link spacing to ensuring sufficient confinement and ductility in the application of RCA is yet not adequately measured. The degree of confinement has a direct impact on post-peak behavior, and flange buckling resistance, making these characteristics crucial. Therefore, an extensive experimental study is required to assess the axial compressive behavior of thin-walled PEC columns constructed with different RCA replacement ratios.

This study involved an experimental program to explore the performance of PEC columns filled with RCA comprehensively. The impacts of RCA replacement ratios on PEC column strength and failure behavior under concentric axial compression were investigated. The influences of link spacing on the capacity of PEC columns filled with RCA were also evaluated. Data-driven insights on sustainable PEC column design are provided by quantitative assessments based on failure modes, peak strain, and ductility indices.

2 Experimental Program

2.1 Descriptions of Column Specimens

The experimental program focused on testing 15 small-scale, thin-walled, partially encased composite (PEC) columns, each with a cross-section of 160 mm × 160 mm and a length of 800 mm. Additionally, three small-scale bare steel columns (H-shaped sections with transverse links at specified spacings) of identical dimensions were tested under axial loading to compare their behavior with the PEC columns. The measured thickness of the steel plates was 3.2 mm, which adhered to the specified dimensions. The key geometric parameters are shown in **Fig. 1**. The primary parameters include the column length (L), the column depth (d), the overall flange width (b_f), the flange width (b), which is defined as half of bf, the center-to-center transverse links spacing (s), and the plate thickness (t). The flange width-to-thickness ratio (b/t) for these columns was designed to be 25, which is lower than the maximum allowable ratio of 32, as specified by CSA S16-24 [48].

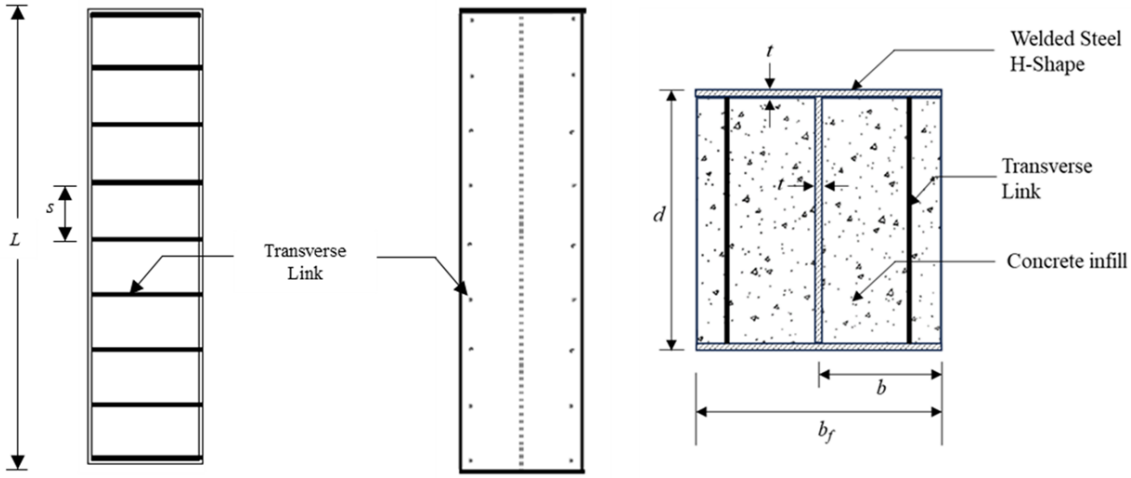

(a) Concrete-side elevation (b) Steel-side elevation (c) Plan view

Fig. 1. The geometric parameters of the PEC column

Table 1. Properties of column specimens

Specimens	Section	Length	Square Link		Steel Yield Stress	Concrete Compressive Strength		RCA (%)
	bf × d × t (mm × mm × mm)	L (mm)	Spacing, s (mm)	(ratio of d)		28 day (MPa)	Test day (MPa)	
SC-A-R0	160 × 160 × 3.2	800	53	0.33d	293	26.2	32.0	0
SC-B-R0	160 × 160 × 3.2	800	80	0.5d	293	26.2	32.0	0
SC-C-R0	160 × 160 × 3.2	800	107	0.67d	293	26.2	32.0	0
SC-A-R25	160 × 160 × 3.2	800	53	0.33d	293	26.3	31.8	25
SC-B-R25	160 × 160 × 3.2	800	80	0.5d	293	26.3	31.8	25
SC-C-R25	160 × 160 × 3.2	800	107	0.67d	293	26.3	31.8	25
SC-A-R50	160 × 160 × 3.2	800	53	0.33d	293	26.1	31.8	50
SC-B-R50	160 × 160 × 3.2	800	80	0.5d	293	26.1	31.8	50
SC-C-R50	160 × 160 × 3.2	800	107	0.67d	293	26.1	31.8	50
SC-A-R75	160 × 160 × 3.2	800	53	0.33d	293	26.0	31.8	75
SC-B-R75	160 × 160 × 3.2	800	80	0.5d	293	26.0	31.8	75
SC-C-R75	160 × 160 × 3.2	800	107	0.67d	293	26.0	31.8	75
SC-A-R100	160 × 160 × 3.2	800	53	0.33d	293	26.1	31.2	100
SC-B-R100	160 × 160 × 3.2	800	80	0.5d	293	26.1	31.2	100
SC-C-R100	160 × 160 × 3.2	800	107	0.67d	293	26.1	31.2	100
SC-A	160 × 160 × 3.2	800	53	0.33d	293	-	-	-
SC-B	160 × 160 × 3.2	800	80	0.5d	293	-	-	-
SC-C	160 × 160 × 3.2	800	107	0.67d	293	-	-	-

To evaluate the influence of link spacing on column behavior, three different spacings were tested: 53 mm (0.33d), 80 mm (0.5d), and 107 mm (0.67d). In all cases, square steel bars with a thickness of 6 mm were used as transverse links. The maximum spacing ratio was 0.67d, the maximum spacing limit

according to CSA S16-24 [48]. Additionally, five different RCA levels were tested for each link spacing to assess the effect of RCA replacement ratio: 0%, 25%, 50%, 75%, and 100%, representing the replacement of NA with RCA in the concrete mixture. 0% RCA indicates concrete cast with NA only, whereas 100% RCA indicates concrete cast fully with RCA. A detailed summary of the column's geometric and material properties can be found in **Table 1**. The columns were labeled using an identifying code in the format "SC"-"A/B/C"-R#. In this system, "A/B/C," denotes the link spacing ratio, where "A," "B," and "C" correspond to link spacing ratios of 0.33*d*, 0.5*d*, and 0.67*d*, respectively, and "R" denotes the replacement ratio of RCAs.

2.2 Material Properties

2.2.1 Steel Plate Properties

Laboratory tests were conducted on the steel plates utilized in the structural steel sections' webs and flanges. A universal testing machine (UTM) with a 2000 kN tensile capability was used to perform tension tests. The average yield strength of the steel plates, as determined by the tension test findings, was 293 MPa. The steel plate's average yield strain was 1465 micro-strain (με), and the average ultimate stress was 431 MPa. The rupture strain was found 336 670 micro-strains (με).

2.2.2 Concrete

Five concrete mixes were prepared for batching the fifteen PEC columns. These mixes were designed to produce concrete with five different RCA replacement ratios. To evaluate the concrete compressive strength, cylinders were cast from each mix. Locally available materials were used to produce concrete. Stone chips of 3/4" downgraded sizes were utilized for natural coarse aggregates and recycled concrete aggregate. The RCA was sourced from crushed concrete cylinder samples previously tested in the Concrete Laboratory, Department of Civil Engineering, BUET. To ensure quality and consistency, only concrete samples cast with natural stone chips as coarse aggregates and known mix proportions and compressive strengths were selected. The average compressive strength of these concrete cylinders was 43.7 MPa, with a standard deviation of 10.5 MPa. These test samples were crushed down to produce RCA. The aggregates were sieved to obtain the 3/4" downgraded portion. Before testing and casting, all coarse aggregates were washed to ensure cleanliness. Additionally, both NA and RCA were pre-soaked for a whole day to address the water absorption of aggregate. Sylhet sands were used for fine aggregate. CEM-II/A-M type cement was used in the concrete mix. The water-cement ratio was kept constant at 0.46 for all the mixes. To guarantee even load distribution in the testing apparatus, a high-strength capping compound was applied to the cylinders prior to testing. All the cylinder's failure mode was the combined crushing of both mortar and stone. The mix proportions and corresponding compressive strength results for all concrete mixes are provided in **Table 2**.

Table 2. The mix ratios and compressive strength of concrete

Mix No	RCA (%)	Cement (kg/m^3)	Fine Aggregate (kg/m^3)	Coarse Aggregate (NA) (kg/m^3)	Coarse Aggregate (RCA) (kg/m^3)	Water (kg/m^3)	Compressive Strength (MPa)
Mix-I	0	366	630	1251	-	168	26.2
Mix-II	25	366	630	938	267	168	26.3
Mix-III	50	366	630	626	535	168	26.1
Mix-IV	75	366	630	313	802	168	26.0
Mix-V	100	366	630	-	1070	168	26.1

In **Table 2**, the compressive strength values were comparable for all the mix designs, and The RCA replacement ratio had very little effect. Many studies have found that using RCA as a replacement for natural coarse aggregate reduces the strength of concrete by 4% to 40% [5,7,49]. However, the strength of concrete with RCA largely depends on the source concrete's strength. If the source concrete strength is higher than the design strength, then concrete with RCA can be compared to concrete made with NA [5,8,44]. Kabir et al. [9] and Malešev et al. [10] also found that using laboratory test samples as RCA did not affect the compressive strength of concrete. The source concrete for RCA in this investigation had a mean strength of 43.7 MPa, which is significantly higher than the 26.2 MPa strength of the

concrete made with NA. This likely explains why no significant reduction in strength was obtained when using RCA in the concrete.

2.3 Test Setup and Data Acquisition System

All the columns were tested using a UTM with a loading capability of 2000 kN in the Structure and Materials Laboratory, Department of Civil Engineering, BUET. The test setup ensured proper end conditions to provide a uniform loading surface for the columns. Two dial gauges were placed in the mid-height of the column in two face directions to measure the lateral deformation. In order to measure the strain of the column, six strain gauges were placed at different positions of the column. The test setup for the concentrically loaded columns is shown in **Fig. 2**. Initially, a loading rate of 0.4 mm/min was used for displacement control. After the peak load, a loading rate of 0.8mm/min was maintained for the remainder of the testing procedure when the load dropped about 90% of the peak load. An electronic data acquisition device was used to record digital readings of axial load and deformation while each specimen was being tested.

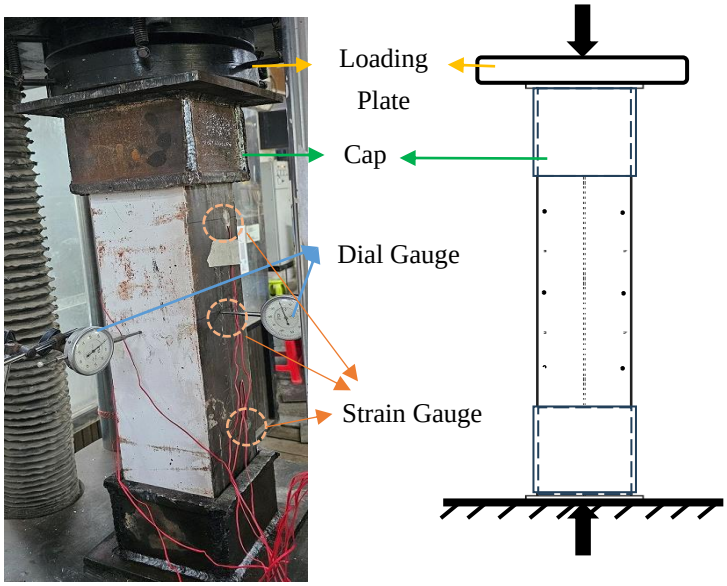

Fig. 2. Test setup for concentric axial load

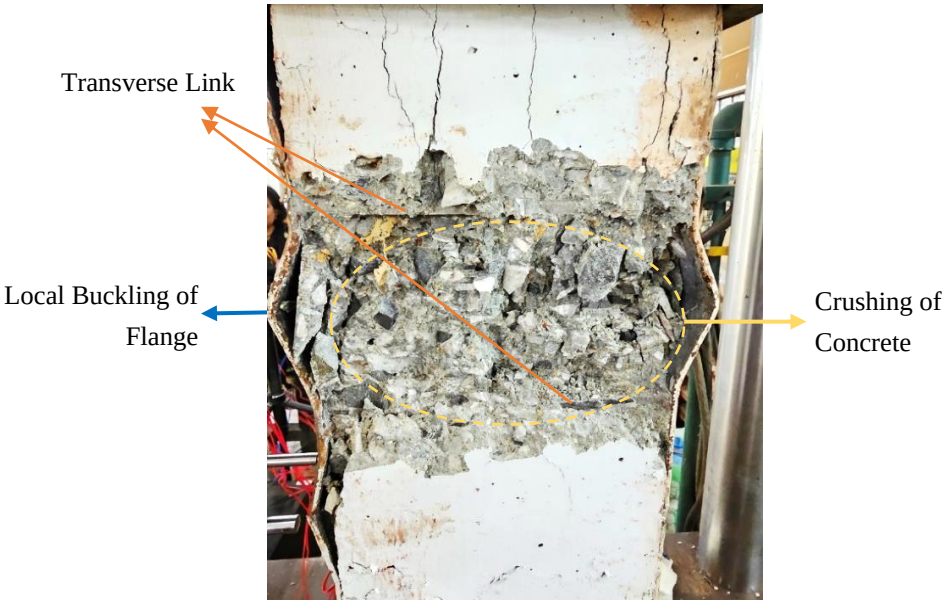

Fig. 3. Typical failure mode of PEC column

3 Results and Discussions

3.1 Failure Modes

a) SC-A-R0 (b) SC-A-R25 (c) SC-A-R50 (d) SC-A-R75

(e) SC-A-R100 (f) SC-B-R0 (g) SC-B-R25 (h) SC-B-R50

Fig. 4. PEC columns after the test (part 1)

All of the columns had the same failure modes. The failure of all PEC columns was caused by a combination of localized steel flange buckling and concrete crushing. A typical failure mode is shown in **Fig. 3**. The PEC column specimens after the test are presented in **Figs. 4** and **5**. The concrete was crushed first, and then the steel flanges buckled locally, causing the failure. In contrast, local buckling of the steel plates (both the web and the flanges) caused the bare steel columns to fail. For all the columns, the flanges yielded before reaching the peak load. Key observations include:

i. In PEC columns with smaller link spacing (s/d = 0.33), concrete between the flanges and web was crushed before reaching the peak load. No local buckling of the flanges occurred before the peak load. The failure was gradual, except in the case of column SC-A-R100. The concrete part of this PEC column was constructed with 100% recycled aggregate. During the test of this column, the loading rate increased rapidly before the peak, and after the peak, the load dropped sharply.

ii. The concrete was also crushed before reaching the peak load in PEC columns with medium link spacing (s/d = 0.5). The failure was gradual. No local buckling of the flanges occurred before the peak load, except in column SC-B-R100, where flange buckling began just before reaching the peak load.

iii. In PEC columns with larger link spacing (s/d = 0.67), concrete crushing occurred before reaching the peak load, followed by local flange buckling. In the test columns with s/d = 0.67, local buckling of the flanges was observed prior to the peak load. The failure was gradual, except for column SC-C-R100, where a rapid load drop occurred after the peak load.

iv. Columns with smaller link spacing exhibited more ductile failure than those with larger ones. Similarly, columns containing up to 50% RCA demonstrated more ductile behavior than those without RCA. However, when the RCA replacement ratio exceeded 50%, the failure became less ductile.

v. In all PEC columns, the flanges buckled outward due to the concrete core. In contrast, the bare steel columns showed both the inward and outward buckling of the flanges.

(i) SC-B-R75 (j) SC-B-R100 (k) SC-C-R0 (l) SC-C-R25

(m) SC-C-R50 (n) SC-C-R75 (o) SC-C-R100

Fig. 5. PEC columns after the test (part 2)

3.2 Axial Load versus Strain Response

A summary of all the load vs. strain curve characteristics can be found in **Table 3**. **Fig. 6** shows the influences of link spacing on the axial load versus strain responses for different RCA replacement ratios. According to link spacing, the samples were divided into three groups: A, B, and C. Their corresponding link spacing to depth ratios (*s/d*) are 0.33, 0.50, and 0.67, respectively. From the figure, initial stiffness was found to be nearly similar for different link spacing. The secant modulus was determined from the initial slope of the axial load versus strain curve. It is the ratio of load and strain at 0.4 P_u [18]. From **Table 3**, the secant modulus for test PEC columns varies from 0.77 to 1.02 kN/με with an average value of 0.91 kN/με. The effect of link spacing on the secant modulus for each RCA replacement ratio is found to be insignificant.

Table 3. Test load summary for columns

Specimens	RCA (%)	Ultimate Load, P_u (kN)	Theoretical Load, P_{th} (kN)	Strain at Peak Load, ε_u (με)	Ductility Index	Secant Modulus (kN/με)
SC-A-R0	0	1216	1021	1885	1.66	0.93
SC-B-R0	0	1171	1009	2074	1.35	1.02
SC-C-R0	0	1135	993	1852	1.33	0.93
SC-A-R25	25	1250	1018	2003	1.78	0.92
SC-B-R25	25	1145	1005	2032	1.44	0.92
SC-C-R25	25	1093	989	2020	1.38	0.96
SC-A-R50	50	1203	1018	2288	1.72	0.88
SC-B-R50	50	1165	1005	2133	1.42	1.01
SC-C-R50	50	1080	989	1996	1.29	0.90
SC-A-R75	75	1178	1018	2294	1.44	0.77
SC-B-R75	75	1158	1005	2174	1.23	0.83
SC-C-R75	75	1101	989	2005	1.23	0.94
SC-A-R100	100	1188	1008	2361	1.44	0.78
SC-B-R100	100	1158	995	2196	1.25	0.93
SC-C-R100	100	1066	979	2029	1.10	0.86
SC-A	-	405	436	1642	1.71	0.42
SC-B	-	391	424	1590	1.35	0.37
SC-C	-	384	408	1568	1.07	0.35

From **Fig. 6**, the post-peak response varies with link spacing for the selected RCA replacement ratio. The post-peak curve gets steeper as the link spacing increases. Therefore, increasing link spacing reduces the ductility of the PEC column constructed with RCA. Reducing the link spacing increases the confinement of the concrete. Therefore, the failure becomes more ductile. Similar behavior was observed for PEC columns constructed with NA.

Fig. 7 illustrates the effects of RCA replacement ratios on the axial load versus strain response for different link spacings. As before, the initial stiffness is nearly consistent across all PEC columns for different RCA ratios. In **Fig. 7(a)** (*s/d* = 0.33), the initial stiffness remains similar for loads up to 600 kN. Beyond this point, the column with 0% RCA shows higher stiffness as compared to that of the column with 100% RCA. **Fig. 7(b)** (*s/d* = 0.5) shows a similar trend, with the column with 0% RCA steepening and the column with 75% RCA becoming milder after 600 kN. In **Fig. 7(c)** (*s/d* = 0.67), the initial stiffness is close up to 700 kN, after which the columns with 0% and 25% RCA become slightly steeper, and the column with 100% RCA again shows a lower initial stiffness. Overall, these variations are minimal, indicating that initial stiffness is mainly independent of the RCA replacement ratio. Notably, the initial stiffness of all PEC columns significantly exceeds that of the bare steel columns.

From the figures, the post-peak responses for Groups A, B, and C are close across the RCA replacement ratio up to 50%. Although reduction of ultimate load is small, the post-peak curve is steeper for columns with 75% and 100% RCA. Therefore, increasing the RCA replacement ratio by more than 50% reduces the ductility and increase the brittleness of the column. Microcracks in RCA and the comparatively weak interfacial transition zone (ITZ) [7, 50] between the new cement paste and residual mortar are the reasons for this increased brittleness. The ITZ between adhered mortar in RCA and new cement paste become porous and less cohesive [51]. This facilitates early crack localization and reduces

fracture energy. The fracture energy reduces significantly at higher RCA replacement ratio [51-52]. As a result, failure becomes more sudden at higher RCA replacement ratio.

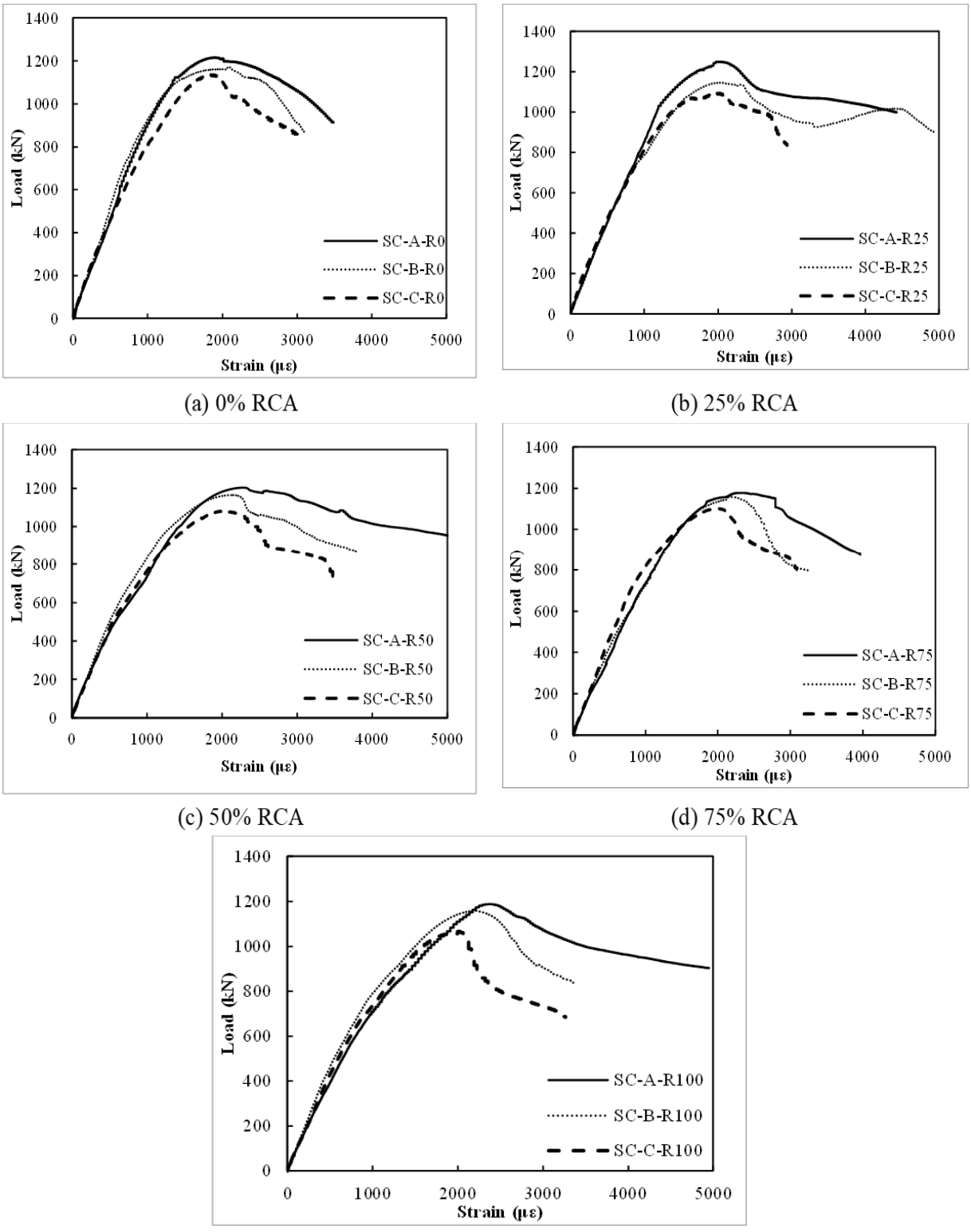

Fig.6. Effects of link spacing on load vs. strain curve

3.3 Strain at Peak Load

Table 3 presents the strain values at peak load (ultimate load) for all columns, while **Fig. 8** summarizes the impacts of link spacing on strain at peak load. The strain at peak load decreases as link

spacing increases. Specifically, for an increase in the *s/d* ratio from 0.33 to 0.67, the strain at peak load decreases by 2%, 13%, 13%, and 14% for RCA replacement ratios of 0%, 50%, 75%, and 100%, respectively. Since all columns exhibit similar initial stiffness, this variation in strain can be attributed to the reduction in peak load as link spacing increases.

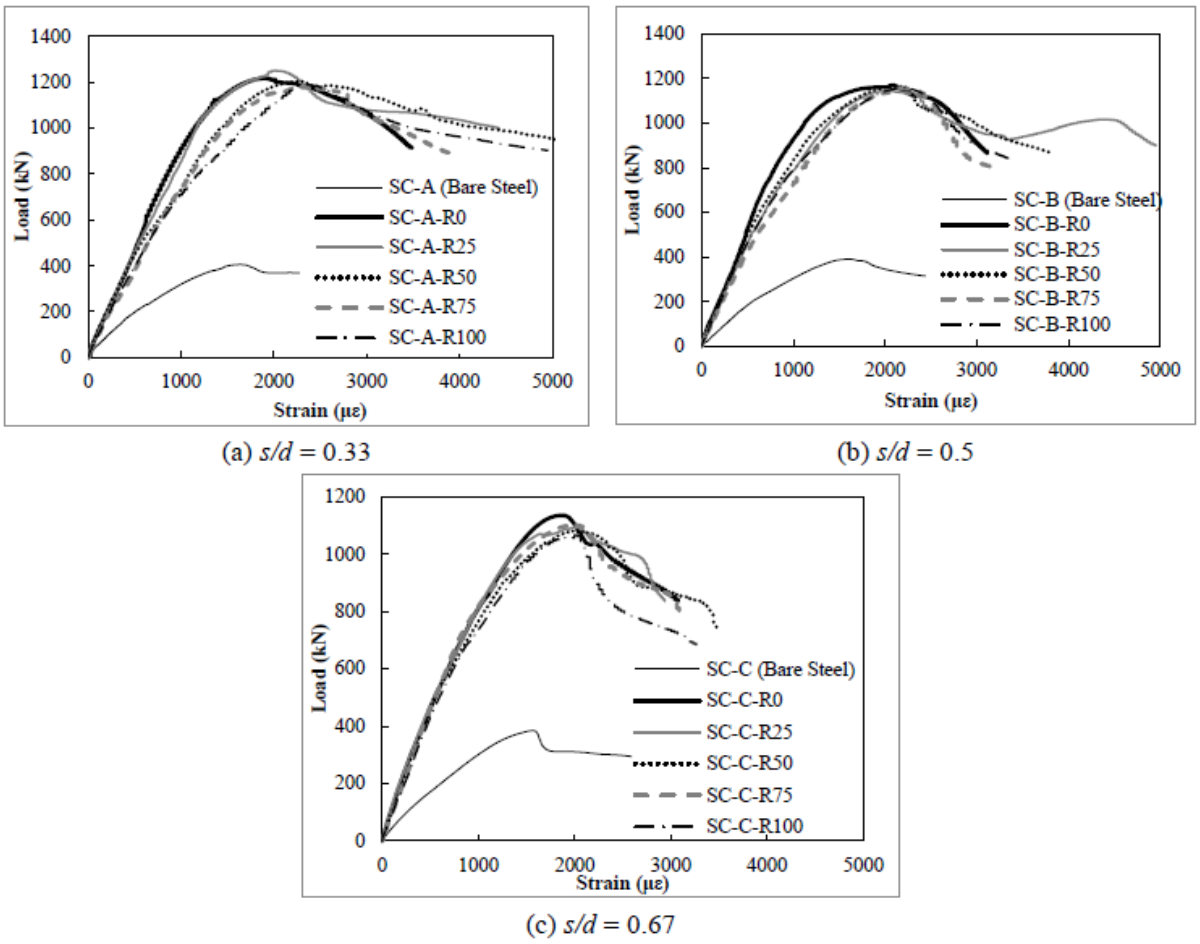

(a) *s/d* = 0.33 (b) *s/d* = 0.5

(c) *s/d* = 0.67

Fig. 7. Effects of link spacing on load vs. strain curve

For the 25% RCA replacement ratio, the strain did not decrease; however, the variations were minimal, within 1%. In the case of SC-B-R0 (*s/d* = 0.5), while the initial stiffness was similar to other columns, the peak strain was 10% higher than that of SC-A-R0 (*s/d* = 0.33). This difference is attributed to the formation of the possible hinge before reaching the peak load in column SC-B-R0.

The effects of the RCA replacement ratio on strain at peak load are summarized in **Fig. 9**. It shows that strain at peak load increases as the RCA replacement ratio increases. The effect is significant for the lower link spacing. For test columns with link spacing 0.33*d*, a 25% increase in peak axial strain is observed as the RCA replacement ratio increases from 0% to 100%. For columns of Group B (*s/d* = 0.5) and Group C (*s/d* = 0.67), the increases in axial strain are 6% and 10%, respectively. Typically, the peak axial strain of the specimen increases as the percentage of RCA replacement ratio increases. This can be attributed to several factors. RCA is comprised of numerous impurities. Such impurities usually reduce the modulus of the concrete, and this modulus diminishes with the increase in the RCA replacement percentage. Consequently, the reduced modulus results in a greater peak strain [53]. For all the PEC columns, strains at the peak load are higher than those for bare steel columns. This is because the composite column portion has higher strength and stiffness than the steel-only part.

3.4 Ultimate Axial Load

The ultimate axial compressive loads for all test columns can be found in **Table 3**. **Fig. 10** summarizes the impacts of link spacing on the ultimate load. Increasing link spacing decreased the axial compression capacity for all five selected RCA replacement ratios. It was expected because transverse

links support the flanges, and increasing the link spacing increases the lateral stiffness of the flanges. It reduces lateral buckling and increases column stability. Increasing the *s/d* ratio from 0.33 to 0.67, the ultimate load decreases by 7%, 13%, 10%, 6%, and 10% for RCA replacement ratios of 0%, 25%, 50%, 75%, and 100%, respectively.

Fig. 11 summarizes the effects of the RCA replacement ratio on the ultimate load for different link spacing. It is observed that the ultimate load decreases as the RCA replacement ratio increases. However, the effect is negligible. For *s/d* = 0.33, using RCA maximum 3% strength reduces (for the column with 75% RCA). A 3% increase in strength was also observed for the column with 25% RCA. For *s/d* = 0.5, using RCA, a maximum of 2% strength reduction is observed. Finally, for *s/d* = 0.67, using RCA, the maximum strength is reduced by 6%. This could be attributed to the compressive strengths of the concrete since the compressive strengths of the concrete for all the columns were comparable.

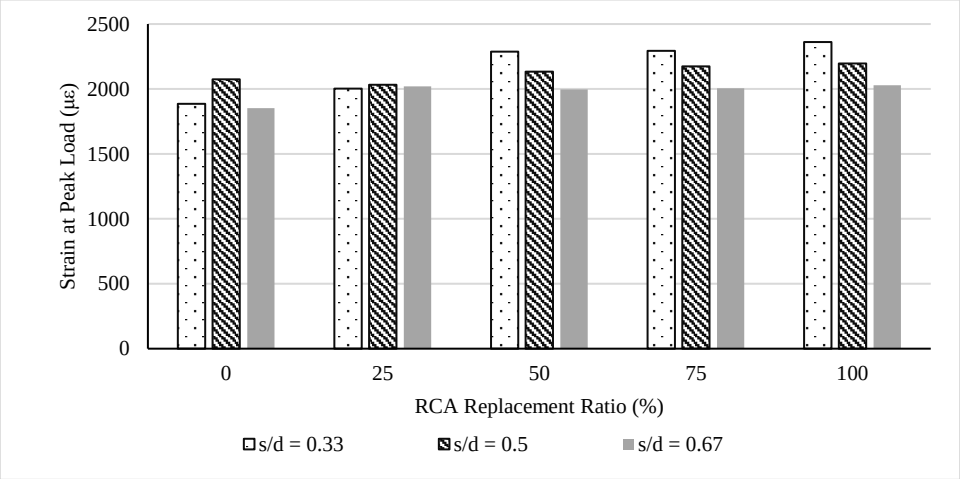

Fig. 8. Effects of the link spacing on the strain at peak load

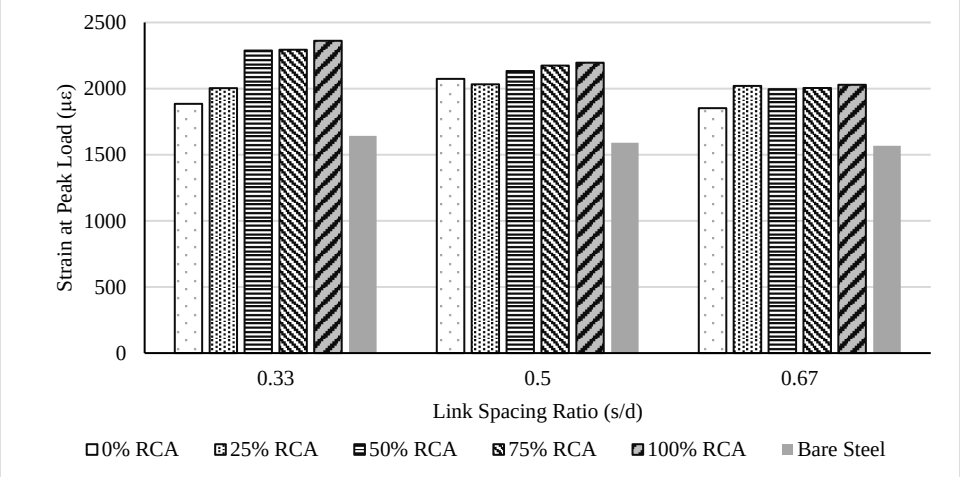

Fig. 9. Effects of the RCA replacement ratio on the strain at peak load

Usually, using RCA degrades concrete strength. Because RCA is often crushed and contains micro-cracks, these micro-cracks can widen under high pressure, leading to a reduction in strength. However, the surface of RCA has a higher roughness, allowing for a stronger bond with the new slurry. Additionally, its porous nature retains some water, which is released during the hydration reaction, enhancing compressive strength. When the negative impact of the deterioration outweighs the strengthening benefits, the strength of the recycled concrete may decrease [54]. In this study, the negative impact of micro-cracks did not govern for concentrically loaded columns.

The ultimate strengths of composite column specimens are also compared with the bare steel column's strength. **Fig. 11** presents the comparison. Concrete results in increased compressive strength for the PEC column constructed with RCA. The PEC column's strengths are about thrice the bare steel

columns. However, this increase reduces as the RCA replacement ratio increases along with the increase in link spacing.

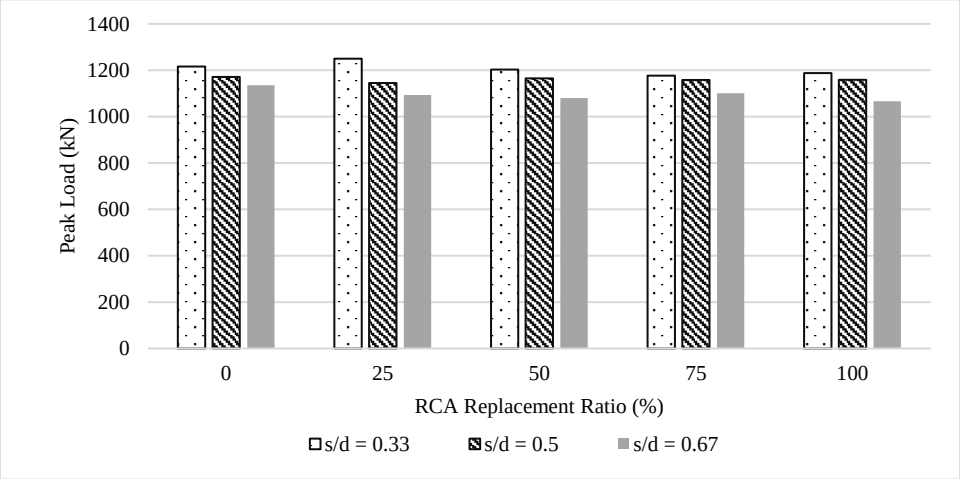

Fig. 10. Effects of the link spacing on the ultimate load

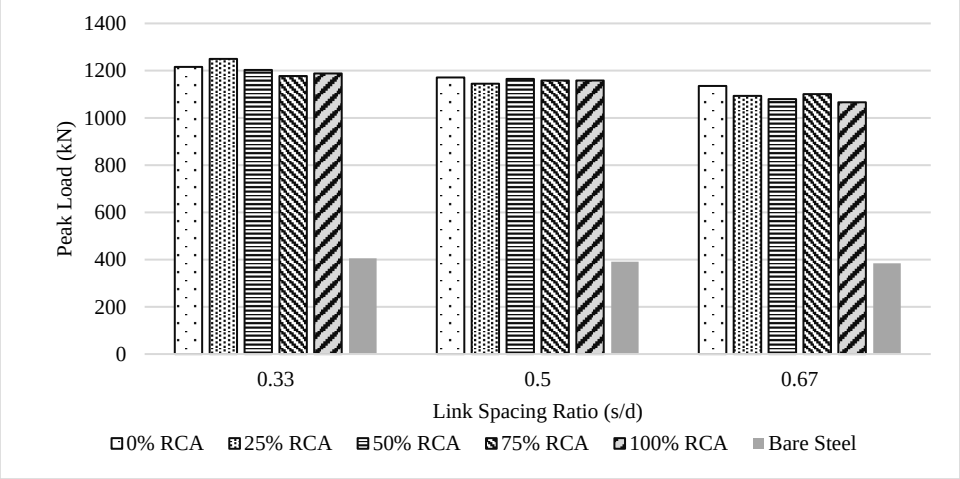

Fig. 11. Effects of the RCA replacement ratio on the ultimate load

3.5 The Ductility Index

The ductility of the columns has been determined using a ductility index (DI) that was introduced by Han et al. [55]. DI is the ratio of the vertical displacement at peak load to the vertical displacement when the load drops to 85% of the peak load. This index shows the efficiency of the composite action between concrete and steel in addition to measuring deformation capacity. According to the test results, lowering link spacing (s/d = 0.33) improves composite interaction and confinement, which raises ductility. On the other hand, because recycled concrete is more brittle, raising the RCA replacement ratio often decreases ductility; however, this degradation is reduced by the confinement effect of closely spaced links.

Table 4. Test load summary for columns

Link Spacing (Ratio of *d*)	RCA Replacement Ratio (%)				
	0	25	50	75	100
0.33 d	1.66	1.78	1.72	1.44	1.44
0.5 d	1.35	1.44	1.42	1.23	1.25
0.67 d	1.33	1.38	1.29	1.23	1.1
% DI Increase (0.67 d to 0.33 *d*)	19.9	22.5	25	14.6	23.6

Table 4 shows that the DI decreases as the link spacing increases. This is because lower link

spacing enhances concrete confinement and reduces the likelihood of steel buckling, making the column more ductile. Consequently, DI is higher for columns with smaller link spacing. The RCA replacement ratio also influences the DI. DI increases when the RCA replacement ratio increases from 0% to 25% due to improved bond and internal curing. However, as the RCA replacement ratio increases further, DI gradually decreases. For link spacing ratios (*s/d*) of 0.33 and 0.5, columns with up to 50% RCA exhibit a higher DI than those with 0% RCA. For a link spacing ratio of 0.67, DI increases up to an RCA ratio of 25%.

This is because RCA has a higher porosity and a lower apparent density, which allows for a closer bond between the concrete and mortar during the hydration and hardening process. It ultimately enhances the ductility of the concrete. However, the RCA micro-cracks increase the concrete's fragility as the replacement ratio increases. Therefore, the DI decreases. Similar observations were also reported by Deng et al. [56].

3.6 Influence on Composite Action and Confinement Performance

In PEC columns, the steel section and the concrete core interact with one another to produce the composite action. This interaction slows the local buckling of steel flanges and increases the axial capacity. According to the experimental findings, link spacing is the primary factor maintaining effective composite behavior, whereas the RCA replacement ratio has a secondary effect that becomes more importance when replacement levels increase.

The reduction of link spacing fostered an increase in the confinement of the concrete core. It restrained lateral deformation of flanges and strengthened the bond between steel section and concrete. Consequently, the occurrence of flange buckling was delayed, and the post-peak load reductions were more gradual in columns with tighter spacing. Columns with smaller reduced link spacing (s*/d* = 0.33) showed enhanced composite action, as evidenced by their higher ductility indices (DI up to 1.78) and increased peak strains (up to 2,361 με for 100% RCA) when compared to columns with larger link spacing (*s/d* = 0.67), which had a maximum DI of 1.38 and peak strains of around 2,029 με. Quantitatively, the DI increased by roughly 20–25% across all RCA replacement ratios when the link spacing (*s/d*) was reduced from 0.67 to 0.33.

The RCA replacement ratio predominantly influenced confinement performance when it exceeded 50%. For the case of *s/d* = 0.33, the DI diminished from 1.78 at 25% RCA to 1.44 at 100% RCA, signifying a 19% decline in confinement efficiency. For *s/d* = 0.67, the similar increase in RCA replacement ratio resulted in a reduction of DI from 1.38 to 1.10 (20% decrease), with local buckling manifesting earlier in the loading process. These findings suggest that the presence of micro-cracks and weaker interfacial bonding in high RCA mixtures compromised the concrete's capacity to effectively restrain the steel flanges. Nevertheless, tighter link spacing alleviated a substantial portion of this negative impact, thereby sustaining composite behavior even at higher RCA levels.

In summation, the performance of confinement and, consequently, composite action was primarily governed by link spacing. RCA replacement ratios up to 50% exert negligible adverse effects when link spacing was small; however, increased RCA levels in conjunction with larger link spacing lead to a measurable reduction in confinement, the early occurrence of flange buckling, and a reduction in ductility.

4 Comparison with Code

Table 3 summarizes the ultimate loads and predicted loads for the columns. The predicted column load was calculated using the CSA S16-24 [48] code. **Table 5** compares the column's capacity with the theoretical capacity predicted by the CSA S16-24 code. For all the PEC columns, the experimental test loads exceeded the predicted theoretical capacities with an average experimental-to-theoretical capacity ratio of 1.15. This indicates that the axial capacity predicting equation of the CSA S16-24 code can be safely used to predict the capacity of the PEC column with concrete containing recycled aggregate.

Across all the RCA replacement ratios, the experimental-to-theoretical capacity ratio was observed to increase as the link spacing decreased, implying enhanced confinement and composite action at closer link spacings. Specifically, the average ratio increased from 1.11 at a spacing of 0.67d to 1.19 at 0.33d.

Therefore, the code is more conservative for the lower link spacing as compared to the higher link spacing. However, the experimental capacities for bare steel columns were lower than the predicted ones, with an average experimental-to-theoretical capacity ratio of 0.93. The lower capacity is due to the presence of initial imperfections in the steel flanges and web, which may have resulted in premature local buckling and lower effective strength.

Table 5. Test load summary for columns

Link Spacing (Ratio of *d*)	RCA Replacement Ratio (%)						Bare Steel
	0	25	50	75	100	Average	
0.33 *d*	1.19	1.23	1.18	1.16	1.18	1.19	0.93
0.5 *d*	1.16	1.14	1.16	1.15	1.16	1.15	0.92
0.67 *d*	1.14	1.11	1.09	1.11	1.09	1.11	0.94

5 Conclusions

An extensive experimental study was conducted to evaluate the effects of RCA on the behavior of thin-walled PEC columns. A total of 15 short PEC columns and three short bare steel columns with similar geometric dimensions were tested. All the columns were loaded under axial concentric load. The test parameters were transverse link spacing and RCA replacement ratio. The RCA was generated from the crushing of the laboratory test samples.

1. All of the PEC columns failed in the same way, with the steel flange buckling locally and the concrete crushing. The failure was started with the crushing of concrete. For smaller link spacing, no local buckling was seen prior to the peak load. However, local buckling was observed prior to the peak load for greater link spacing, indicating enhanced confinement at lower link spacing. The failure modes of the bare steel were local buckling of the flange and web.
2. The link spacings and RCA replacement ratio did not affect the initial stiffness significantly. However, the initial stiffnesses of the PEC columns were significantly higher than that of bare steel columns. Increasing the RCA replacement ratio increased the strain at peak load, particularly for columns with lower link spacing, due to the presence of impurities in RCA.
3. Post-peak response was affected by the RCA replacement ratio. After 50% RCA, the response becomes steeper. For the columns with an RCA replacement ratio higher than 50%, the ductility index was reduced than that of the column with 0% RCA. About 20% decrease in DI was found at higher levels of RCA (75% and 100% RCA). This is due to the presence of micro-cracks in the RCA. The columns with 25% RCA had the highest ductility index.
4. An increase in link spacing decreased the ultimate load for all columns. As the *s/d* ratio increased from 0.33 to 0.67, the ultimate load was observed to decrease by 6% to 13% and the ductility index to decrease by approximately 20–25%. This was anticipated because closer link spacing enhances lateral stiffness, mitigates flange buckling, and improves the stability of the columns.
5. The RCA replacement ratio had a minimal effect on the ultimate load of the column. A maximum 6% load was reduced as RCA was used in the PEC column since the compressive strength of concrete with RCA was comparable with that of conventional concrete. The higher surface roughness and porous nature of RCA improve bonding with slurry and enhance compressive strength. However, the capacity of all the PEC columns was about two times higher than that of the bare steel column.
6. All columns surpassed the capacity predicted by the CSA S16-24 code, suggesting that the capacity equation provided by the code can safely calculate the capacity of PEC columns containing RCA.

These findings emphasize that suitable link spacing can preserve composite action and confinement, which allows the sustainable use of RCA (up to 50%) in PEC columns without compromising ultimate axial capacity or ductility.

Acknowledgement

The authors are grateful to the Department of Civil Engineering, Bangladesh University of Engineering and Technology for the research facilities. The authors also gratefully acknowledge McDonald Steel Building Products Limited for their support in the fabrication of the columns.

Funding Statement

The research was funded by the Committee for Advanced Studies and Research, Bangladesh University of Engineering and Technology. McDonald Steel Building Products Limited supplied and fabricated the steel required to prepare the column specimens.

CRediT authorship contribution statement

Meftahul Ahsan: Conceptualization, Investigation, Methodology, Formal analysis, Writing – original draft. **Md. Tanzil Hawlader**: Investigation, Formal analysis. **Mahbuba Begum**: Conceptualization, Supervision, Writing – review & editing.

Conflicts of interest:

The authors declare that they have no conflicts of interest to report regarding the present study.

References

[1] Tam VWY, Soomro M, Evangelista ACJ. A review of recycled aggregate in concrete applications (2000–2017). Construction and Building Materials 2018; 172: 272–92. https://doi.org/10.1016/j.conb uildmat.2018.03.240.
[2] Silva RV, de Brito J, Dhir RK. Availability and processing of recycled aggregates within the construction and demolition supply chain: A review. Journal of Cleaner Production 2017; 143: 598–614. https://doi.org/10.1016/j.jclepro.2016.12.070.
[3] Hossain MU, Poon CS, Lo IMC, Cheng JCP. Comparative environmental evaluation of aggregate production from recycled waste materials and virgin sources by LCA. Resources, Conservation and Recycling 2016; 109: 67–77. https://doi.org/10.1016/j.resconrec.2016.02.009.
[4] De Andrade Salgado F, De Andrade Silva F. Recycled aggregates from construction and demolition waste towards an application on structural concrete: A review. Journal of Building Engineering 2022; 52: 104452. https://doi.org/10.1016/j.jobe.2022.104452.
[5] McNeil K, Kang TH-K. Recycled Concrete Aggregates: A Review. International Journal of Concrete Structures and Materials 2013; 7: 61–9. https://doi.org/10.1007/s40069-013-0032-5.
[6] Singh R, Nayak DK, Kumar R, Kumar V. Study on Coarse Recycled Concrete Aggregate. Civil Engineering and Architecture 2022; 10: 2500–23. https://doi.org/10.13189/cea.2022.100621.
[7] Verian KP, Ashraf W, Cao Y. Properties of recycled concrete aggregate and their influence in new concrete production. Resources, Conservation and Recycling 2018; 133: 30–49. https://doi.org/10.1016/j.resconrec.2018.02.005.
[8] Tabsh SW, Abdelfatah AS. Influence of recycled concrete aggregates on strength properties of concrete. Construction and Building Materials 2009; 23: 1163–7. https://doi.org/10.1016/j.conbuildmat.2008.06.007.
[9] Kabir S, Al-Shayeb A, Khan IM. Recycled Construction Debris as Concrete Aggregate for Sustainable Construction Materials. Procedia Engineering 2016; 145: 1518–25. https://doi.org/10.1016/j.pr oeng.2016.04.191.
[10] Malešev M, Radonjanin V, Marinkovic S. Recycled Concrete as Aggregate for Structural Concrete Production. Sustainability 2010; 2. https://doi.org/10.3390/su2051204.
[11] Tremblay R, Massicotte B, Filion I, Maranda R. Experimental study on the behaviour of partially encased composite columns made with light welded H steel shapes under compressive axial loads. Proceedings of the SSRC Annual Technical Meeting 1998; Atlanta, 195–204.
[12] Chicoine T, Tremblay R, Massicotte B, Mehmet Y, Ricles J, Lu L-W. Test programme on partially-encased built up three-plate composite columns. École Polytechnique; 2000.
[13] Chicoine T, Tremblay R, Massicotte B, Ricles JM, Lu L-W. Behavior and strength of partially encased composite columns with built-up shapes. Journal of Structural Engineering 2002; 128: 279–88. https://doi.org/10.1061/(ASCE)0733-9445(2002)128:3(279)
[14] Chicoine T, Massicotte B, Tremblay R. Long-term behavior and strength of partially encased composite columns made with built-up steel shapes. Journal of Structural Engineering 2003; 129: 141–50. https://doi.org/10.1061/(ASCE)0733-9445(2003)129:2(141)
[15] Zhao GT, Feng C. Axial Ultimate Capacity of Partially Encased Composite Columns. Applied Mechanics

and Materials 2012; 166–169: 292–5. https://doi.org/10.4028/www.scientific.net/AMM.166-169.292.
[16] Bouchereau R, Toupin JD. Étude du comportement en compression-flexion des poteaux mixtes partiellement enrobés. Report EPM/GCS 2003 2003; 3.
[17] Oh M-H, Ju Y-K, Kim M-H, Kim S-D. Structural Performance of Steel-Concrete Composite Column Subjected to Axial and Flexural Loading. Journal of Asian Architecture and Building Engineering 2006; 5: 153–60. https://doi.org/10.3130/jaabe.5.153.
[18] Prickett BS, Driver RG. Behaviour of partially encased composite columns made with high performance concrete. AB, Canada: Department of Civil and Environmental Engineering, University of Alberta; 2006.
[19] Qian Z, Wang J, Liu Y, Xu Q. Axial compressive performance of partially encased steel-concrete composite stub columns filled with lightweight aggregate concrete. Engineering Structures 2023; 291: 116422. https://doi.org/10.1016/j.engstruct.2023.116422.
[20] Wang J, Hu P, Liu Y, Qian Z, Hu C, Zhang H. Axial compressive behavior of the PEC slender columns with lightweight aggregate concrete. Journal of Constructional Steel Research 2023; 211: 108206. https://doi.org/10.1016/j.jcsr.2023.108206.
[21] Pereira MF, Nardin SD, Debs ALHCE. Structural behavior of partially encased composite columns under axial loads. Steel and Composite Structures 2016; 20: 1305–22. https://doi.org/10.12989/SCS.2016.20.6.1305.
[22] Chen Y, Wang T, Yang J, Zhao X. Test and numerical simulation of partially encased composite columns subject to axial and cyclic horizontal loads. International Journal of Steel Structures 2010; 10: 385–93. https://doi.org/10.1007/BF03215846
[23] Ebadi-Jamkhaneh M, Kafi M. Experimental and Numerical Investigation of Octagonal Partially Encased Composite Columns Subject to Axial and Torsion Moment Loading. Civil Engineering Journal 2017; 3: 939–55. https://doi.org/10.28991/cej-030927.
[24] Ebadi-Jamkhaneh M, Kafi M. Experimental and Numerical Study of Octagonal Composite Column Subject to Various Loading. Periodica Polytechnica Civil Engineering 2018; 62: 413–22. https://doi.org/10.3311/PPci.11334.
[25] Ebadi-Jamkhaneh M, Kafi M. Equalizing Octagonal PEC Columns with Steel Columns: Experimental and Theoretical Study. Practice Periodical on Structural Design and Construction 2018; 23(3): 04018012. https://doi.org/10.1061/(ASCE)SC.1943-5576.0000375.
[26] Ebadi-Jamkhaneh M, Kafi M., Kheyroddin A. Behavior of partially encased composite members under various load conditions: Experimental and analytical models. Advances in Structural Engineering 2018; 22(1): 94-111. https://doi.org/10.1177/1369433218778725
[27] Deng X, Dastfan M, Driver RG. Behaviour of Steel Plate Shear Walls with Composite Columns. Structures Congress 2008, Vancouver, British Columbia, Canada: American Society of Civil Engineers 2008; 1–10. https://doi.org/10.1061/41016(314)100.
[28] Dastfan M, Driver R. Large-Scale Test of a Modular Steel Plate Shear Wall with Partially Encased Composite Columns. Journal of Structural Engineering 2016; 142: 04015142. https://doi.org/10.1061/(ASCE)ST.1943-541X.0001424.
[29] Dastfan M, Driver R. Test of a Steel Plate Shear Wall with Partially Encased Composite Columns and RBS Frame Connections. Journal of Structural Engineering 2018; 144: 04017187. https://doi.org/10.1061/(ASCE)ST.1943-541X.0001954.
[30] Yu J, Yu H, Feng X, Dang C, Hou T, Shen J. Behaviour of steel plate shear walls with different types of partially-encased H-section columns. Journal of Constructional Steel Research 2020; 170: 106123. https://doi.org/10.1016/j.jcsr.2020.106123.
[31] Yin Z, Huang Z, Zhang H. Experimental Study on Steel Plate Shear Walls with Partially Encased Composite Columns Composed of Thin Steel Plate. KSCE Journal of Civil Engineering 2023; 27: 1118–35. https://doi.org/10.1007/s12205-023-0017-0.
[32] Chicoine T, Tremblay R, Massicotte B. Finite element modelling and design of partially encased composite columns. Steel and Composite Structures 2002; 2(3):171-194. http://dx.doi.org/10.12989/scs.2002.2.3.171
[33] Begum M, Driver RG, Elwi AE. Finite-element modeling of partially encased composite columns using the dynamic explicit method. Journal of Structural Engineering 2007; 133: 326–34. https://doi.org/10.1061/(ASCE)0733-9445(2007)133:3(326)
[34] Begum M, Driver RG, Elwi AE. Behaviour of partially encased composite columns with high strength concrete. Engineering Structures 2013; 56: 1718–27. https://doi.org/10.1016/j.engstruct.2013.07.040
[35] Begum M, Driver R, Elwi A. Parametric study on eccentrically-loaded partially encased composite columns under major axis bending. Steel and Composite Structures 2015; 19: 1299–319. https://doi.org/10.12989/scs.2015.19.5.1299.
[36] Song Y-C, Wang R-P, Li J. Local and post-local buckling behavior of welded steel shapes in partially encased composite columns. Thin-Walled Structures 2016; 108: 93–108. https://doi.org/10.1016/j.tws.2016.08.003.
[37] Wang H, Li J, Song Y. Numerical study and design recommendations of eccentrically loaded partially

encased composite columns. International Journal of Steel Structures 2019; 19: 991–1009. https://doi.or g/10.1007/s13296-018-0179-7
[38] Ali S, Begum M. Load-moment interaction diagrams of slender partially encased composite columns. Malaysian Journal of Civil Engineering 2013; 25(2). https://doi.org/10.11113/mjce.v25.15856
[39] Begum M, Ghosh D. Simulations of PEC columns with equivalent steel section under gravity loading. Steel and Composite Structures 2014; 16: 305–23. https://doi.org/10.12989/scs.2014.16.3.305.
[40] Wu B, Zhao X-Y, Zhang J-S. Cyclic behavior of thin-walled square steel tubular columns filled with demolished concrete lumps and fresh concrete. Journal of Constructional Steel Research 2012; 77: 69–81. https://doi.org/10.1016/j.jcsr.2012.05.003.
[41] Wu B, Zhao XY, Zhang JS, Liu QX. Seismic Tests on Square Thin-Walled Steel Tubular Columns Filled with Demolished Concrete Lumps. Key Engineering Materials 2012; 517: 958–67. https://doi.org/10.4028/www.scientific.net/KEM.517.958.
[42] Wu B, Lin L, Zhao J, Yan H. Creep behavior of thin-walled circular steel tubular columns filled with demolished concrete lumps and fresh concrete. Construction and Building Materials 2018; 187: 773–90. https://doi.org/10.1016/j.conbuildmat.2018.07.222.
[43] Wu B, Li W-F, Zhao X-Y. Behavior of slender square steel tubular columns filled with fresh concrete and demolished concrete lumps. Procedia Engineering 2017; 210: 196–202. https://doi.org/10.1016/j.pro eng.2017.11.066.
[44] Wu B, Jian S-M, Zhao X-Y. Structural behavior of steel-concrete partially encased composite columns containing demolished concrete lumps under axial compression. Engineering Structures 2019; 197: 109383. https://doi.org/10.1016/j.engstruct.2019.109383
[45] Wang Y, Chen J, Geng Y. Testing and analysis of axially loaded normal-strength recycled aggregate concrete-filled steel tubular stub columns. Engineering Structures 2015; 86: 192–212. https://doi.org/10.1016/j.engstruct.2015.01.007.
[46] Yang Y-F, Han L-H. Compressive and flexural behaviour of recycled aggregate concrete filled steel tubes (RACFST) under short-term loadings. Steel and Composite Structures 2006; 6: 257–84. https://doi.or g/10.12989/scs.2006.6.3.257.
[47] Zhao X-Y, Wu B, Wang L. Structural response of thin-walled circular steel tubular columns filled with demolished concrete lumps and fresh concrete. Construction and Building Materials 2016; 129: 216–42. https://doi.org/10.1016/j.conbuildmat.2016.10.099.
[48] CSA Group. CSA S16-24, Limit States Design of Steel Structures. Toronto, ON: Canadian Standards Association; 2024.
[49] Tran DVP, Allawi A, Albayati A, Cao TN, El-Zohairy A, Nguyen YTH. Recycled Concrete Aggregate for Medium-Quality Structural Concrete. Materials 2021; 14: 4612. https://doi.org/10.3390/ma14164612.
[50] Muhammad F, Harun M, Ahmed A, Kabir N, Khalid HR, Hanif A. Influence of bonded mortar on recycled aggregate concrete properties: A review. Construction and Building Materials 2024; 432: 136564. https://doi.org/10.1016/j.conbuildmat.2024.136564.
[51] Hadjari M, Marouf H, Dahou Z, Maherzi W. Investigation of the Mechanical and Fracture Properties of Recycled Aggregate Concrete. Buildings 2025; 15: 1155. https://doi.org/10.3390/buildings15071155
[52] Li T, Xiao J, Zhang Y, Chen B. Fracture behavior of recycled aggregate concrete under three-point bending. Cement and Concrete Composites 2019; 104: 103353. https://doi.org/10.1016/j.cemconcomp.2019.103353.
[53] Xiao J, Huang Y, Yang J, Zhang Ch. Mechanical properties of confined recycled aggregate concrete under axial compression. Construction and Building Materials 2012; 26: 591–603. https://doi.org/10.1016/j.conbuildmat.2011.06.062.
[54] Wang C, Cheng L, Ying Y, Yang F. Utilization of all components of waste concrete: Recycled aggregate strengthening, recycled fine powder activity, composite recycled concrete and life cycle assessment. Journal of Building Engineering 2024; 82: 108255. https://doi.org/10.1016/j.jobe.2023.108255.
[55] Han L-H, Ren Q-X, Li W. Tests on stub stainless steel–concrete–carbon steel double-skin tubular (DST) columns. Journal of Constructional Steel Research 2011; 67: 437–52. https://doi.org/10.1016/j.jcsr.2010.09.010.
[56] Deng Z, Liu B, Ye B, Xiang P. Mechanical behavior and constitutive relationship of the three types of recycled coarse aggregate concrete based on standard classification. Journal of Material Cycles and Waste Management 2019; 22. https://doi.org/10.1007/s10163-019-00922-5.